HNF1A regulates oxaliplatin resistance in pancreatic cancer by targeting 53BP1

RENPENG XIA[1,2*], CHONGHUI HU[2*], YUANCHENG YE[1,2*], XIANG ZHANG[3], TINGTING LI[4], RIHUA HE[2,5], SHANGYOU ZHENG[2], XIAOFENG WEN[6] and RUFU CHEN[1,2]

[1]The Second School of Clinical Medicine, Southern Medical University, Guangzhou, Guangdong 510515; [2]Department of Pancreas Center, Guangdong Provincial People's Hospital (Guangdong Academy of Medical Sciences), Southern Medical University, Guangzhou, Guangdong 510080; [3]Department of Gastrointestinal Surgery, The First Affiliated Hospital of Sun Yat-Sen University, Guangzhou, Guangdong 510120; [4]School of Medicine, South China University of Technology, Guangzhou, Guangdong 510006; [5]Graduate School, Shantou University Medical College, Shantou, Guangdong 515041; [6]Department of Colorectal Surgery, The Sixth Affiliated Hospital, Sun Yat-sen University, Guangzhou, Guangdong 510655, P.R. China

Received August 23, 2022; Accepted January 27, 2023

DOI: 10.3892/ijo.2023.5493

Abstract. DNA double-strand break repair is critically involved in oxaliplatin resistance in pancreatic ductal adenocarcinoma (PDAC). Hepatocyte nuclear factor 1 homeobox A (HNF1A) has received increased attention regarding its role in cancer progression. The present study explored the role of HNF1A in oxaliplatin resistance in PDAC. The results revealed that HNF1A expression was negatively associated with oxaliplatin chemoresistance in PDAC tissues and cell lines. HNF1A inhibition promoted the proliferation, colony formation and stemness of PDAC cells, and suppressed their apoptosis. Furthermore, HNF1A inhibition switched nonhomologous end joining to homologous recombination, thereby enhancing genomic stability and oxaliplatin resistance. Mechanistically, HNF1A transcriptionally activates p53-binding protein 1 (53BP1) expression by directly interacting with the 53BP1 promoter region. Upregulation of HNF1A and 53BP1 induced significant inhibition of PDAC growth and oxaliplatin resistance in patient-derived PDAC xenograft models and orthotopic models. In conclusion, the findings of the present study suggested that HNF1A/53BP1 may be a promising PDAC therapeutic target for overcoming oxaliplatin resistance.

Correspondence to: Professor Xiaofeng Wen, Department of Colorectal Surgery, The Sixth Affiliated Hospital, Sun Yat-sen University, 26 Erheng Road, Guangzhou, Guangdong 510655, P.R. China
E-mail: wenxf6@mail.sysu.edu.cn

Professor Rufu Chen, Department of Pancreas Center, Guangdong Provincial People's Hospital (Guangdong Academy of Medical Sciences), Southern Medical University, 106 Second Zhongshan Road, Guangzhou, Guangdong 510080, P.R. China
E-mail: chenrufu@gdph.org.cn

*Contributed equally

Abbreviations: PDAC, pancreatic ductal adenocarcinoma; HR, homologous recombination; NHEJ, nonhomologous end-joining; 53BP1, p53-binding protein 1; DSB, DNA double strand break; CCK-8, Cell Counting Kit-8; IF, immunofluorescence

Key words: PDAC, hepatocyte nuclear factor 1 homeobox A, p53-binding protein 1, chemoresistance, DNA repair

Introduction

Pancreatic adenocarcinoma (PDAC) is a leading cause of cancer-related mortality worldwide, with a 5-year survival rate of ~5% (1). Because of delayed diagnosis and early metastasis, only 15-20% of patients have a chance to undergo surgery (2). Therefore, systemic chemotherapy is applied in the majority of patients with locally advanced and metastatic PDAC. The first-line systemic chemotherapies for locally advanced or metastatic PDAC include fluorouracil, leucovorin, irinotecan and oxaliplatin (FOLFIRINOX) and gemcitabine plus nab-paclitaxel (3), both of which have been proven to improve the clinical outcome. FOLFIRINOX is associated with a better clinical outcome but has greater toxicity than gemcitabine, which limits its application in patients with poor performance status (4). However, oxaliplatin can be offered as a replacement therapy for these patients as well (5). Unfortunately, after several weeks of chemotherapy, an initially sensitive tumor may become resistant to platinum-based chemotherapy (6). Therefore, there remains an urgent need for novel therapies to overcome resistance and increase the efficacy of oxaliplatin in PDAC treatment.

DNA double-strand breaks (DSBs) are modified through either homologous recombination (HR) or nonhomologous end joining (NHEJ) pathways. The choice of these two DSB repair pathways is determined by a number of factors, such as DSB end structure and cell cycle. The DNA damage response

protein p53-binding protein 1 (53BP1) regulates these DSB repair pathways; it promotes NHEJ and suppresses HR (7).

Hepatocyte nuclear factor 1 homeobox A (HNF1A) is enriched in the liver, and is expressed in the kidney, intestine and pancreas (8). Previous studies have shown that HNF1A regulates lipid and carbohydrate metabolism in hepatocytes and pancreatic islet cells (9,10). HNF1A gene variants have been reported to cause maturity-onset diabetes of the young, type 3 (MODY3) and are associated with the risk of PDAC (11,12). In addition, previous studies (13-15) have shown that HNF1A regulates gemcitabine resistance by targeting ABCB1, and that it serves a tumor suppressor role in PDAC (14). HNF1A has been proven to regulate a series of genes associated with glucose metabolism and multidrug resistance proteins to mediate oxaliplatin resistance (16). However, to the best of our knowledge, the role of HNF1A in oxaliplatin chemotherapy resistance in PDAC has not been determined. The present study explored the effect of HNF1A on oxaliplatin resistance in PDAC.

Materials and methods

Patients and clinical samples. A total of 76 locally advanced PDAC specimens were collected from patients (median age, 61.2 years; age range, 32-79 years; 43 male patients, 33 female patients) who received a platinum-based chemotherapy program at Guangdong Provincial People's Hospital and Sun Yat-sen Memorial Hospital (both Guangzhou, China) between July 2015 and June 2021. Patients with locally advanced PDAC underwent laparoscopic biopsy or endoscopic ultrasound-guided sample acquisition from a solid pancreatic mass. The samples were confirmed as PDAC by two certified pathologists. Patients were included if they i) were 18-80 years of age; ii) had advanced PDAC stage III or IV, according to the pathology results; iii) had received oxaliplatin chemotherapy; and iv) had provided written informed consent. Patients were excluded if they i) had received other specific pancreatic cancer treatments (surgery, preoperative chemotherapy or chemoradiation); ii) had a pathologic diagnosis of a benign tumor; iii) had a history of other malignancies; or iv) had a mental illness. In accordance with the Guangdong Provincial People's Hospital's Protection of Human Subjects Committee (approval no. KY-H-2022-011-01), the protocol was approved, and all of the patients provided written informed consent before the biopsy sample collection. Progression-free survival (PFS) was measured from the date of chemotherapy to the occurrence of an event (progressive disease, death or diagnosis of a second malignant neoplasm). The response of oxaliplatin chemotherapy was assessed 4 months after the start of chemotherapy, complete response (CR) and partial response (PR) were classified as oxaliplatin-sensitive (35 cases), while stable disease (SD) and progressive disease (PD) were classified as oxaliplatin-resistant (41 cases).

Cell culture. MiaPaCa-2 [cat. no. CRM-CRL-1420; Research Resource Identifier (RRID): CVCL_0428] and Panc-1 (cat. no. CRL-1469MET; RRID: CVCL_A4BT) cells were obtained from the American Type Culture Collection. Cells were maintained in Dulbecco's modified Eagle's medium (DMEM; Gibco; Thermo Fisher Scientific, Inc.) supplemented with 10% fetal bovine serum (Gibco; Thermo Fisher Scientific, Inc.), 100 U/ml penicillin and 100 mg/ml streptomycin, and were cultured at 37˚C in a humidified atmosphere with 5% CO_2.

Construction of oxaliplatin-resistant cell lines. Panc-1 and MiaPaCa-2 cells with resistance to oxaliplatin were named Panc-1-R and MiaPaCa-2-R, respectively. First, 2 mg/ml oxaliplatin (cat. no. S1224; Selleck Chemicals, dissolved to storage concentration with DMSO and diluted to working concentrations with DMEM) solution was added to Panc-1 and MiaPaCa-2 cells and incubated at 37˚C for 24 h; subsequently, the medium was replaced with oxaliplatin-free medium and cell proliferation was observed using a CCK-8 assay (cat. no. K1018; APExBIO Technology LLC). Panc-1 and MiaPaCa-2 cells were repeatedly stimulated in this manner until proliferation was no longer inhibited. The concentration of oxaliplatin was then increased to 3, 4, 6, 8 and 10 mg/ml to develop Panc-1-R and MiaPaCa-2-R cells.

Panc-1 and MiaPaCa-2 cells ($5x10^3$/well) were seeded in 96-well plates to detect the drug response. After 24 h, fresh medium containing oxaliplatin at a gradient concentration of 0, 0.001, 0.01, 0.1, 1, 10, 100 and 1,000 μM was added to the cells and incubated for 72 h at 37˚C. The cells were then incubated with 10 μl CCK-8 solution at 37˚C for 2 h and the absorbance was measured using a microplate reader (Thermo Fisher Scientific, Inc.) at 450 nm. The degree of drug response for tumor cells was determined by the half-maximal inhibitory concentration (IC_{50}), which was calculated with GraphPad Prism 8.0 (Dotmatics).

Immunohistochemistry (IHC). Paraffin-embedded human tissue samples (5 μm) were deparaffinized using the following steps: 3x10 min in xylol, 2x5 min in 100% ethanol, 1x5 min in 95% ethanol, 1x5 min in 85% ethanol and 1x5 min in 75% ethanol. Antigen retrieval was performed in a microwave oven with sodium citrate buffer (0.01 M, pH 6.0; Beyotime Institute of Biotechnology) for 20 min. Subsequently, 3% H_2O_2 was used to remove endogenous peroxidase for 15 min at room temperature. Slides were incubated with normal goat serum (Beyotime Institute of Biotechnology) for 30 min at room temperature to block unspecific background staining. The tissues were then incubated at 4˚C overnight with primary rabbit anti-human antibodies against HNF1A (1:200; cat. no. ab96777), Ki-67 (1:200; cat. no. ab15580), 53BP1 (1:200; cat. no. ab87097) and γ-H2AX (1:200; cat. no. ab81299) (all from Abcam), followed by incubation withbiotin-conjugated secondary antibodies at room temperature for 20 min. Subsequently, each slide was incubated at room temperature with streptavidin-HRP conjugate (Beyotime Institute of Biotechnology) for 20 min. The staining procedure was performed using a DAB Kit (Beyotime Institute of Biotechnology) according to the manufacturer's instructions. Mayer's hematoxylin (Beyotime Institute of Biotechnology) was used for counterstaining all slides at room temperature for 20-30 sec. Staining was observed and images were captured with an inverted microscope (Olympus IX-71; Olympus Corporation).

A semi-quantitative assessment of HNF1A expression levels was performed using the immunoreactive score and staining intensity. The scoring of the staining intensity was as follows: 0, no staining; 1, light; 2, intermediate; and 3,

strong. The scoring of the proportion of HNF1A- or 53BP1 positive-cells was as follows: 1, <25%; 2, ≥25-<50%; 3, ≥50-<75%; and 4, ≥75-100%. The final score was obtained by multiplying the staining intensity and the proportion of positively stained cells. Cases with a score of >4 were considered to have high expression, whereas those with a score of ≤4 were considered to have low expression. Discrepancies in staining were re-evaluated by two pathologists until a consensus was reached after the staining was professionally assessed using the scoring criteria.

RNA extraction and reverse transcription-quantitative PCR (RT-qPCR). Total RNA from tissues and cells was isolated by TRIzol® reagent (Invitrogen; Thermo Fisher Scientific, Inc.) according to the manufacturer's instructions and was reverse transcribed using HiScript Reverse Transcriptase (cat. no. R101-01; Vazyme Biotech Co., Ltd.). qPCR was performed using the SYBR Premix Ex Taq™ kit (cat. no. DRR420A; Takara Bio, Inc.), GAPDH was used as the universal control. RT-qPCR was conducted using the CFX96 Touch Real-Time PCR detection system (Bio-Rad Laboratories, Inc.). The thermocycling conditions include initial denaturation at 95˚C for 30 sec, followed by 35 cycles at 95˚C for 5 sec, annealing at 60˚C for 30 sec. All reactions were examined in technical triplicate. Gene expression analysis was performed using the $2^{-\Delta\Delta Cq}$ method (17). The primer sequences are listed in Table SI.

Establishment of knockdown and overexpression cell lines. Human HNF1A and 53BP1 coding sequences were subcloned into the pMKO.1-puro vector (Guangzhou IGE Biotechnology Ltd.) and the empty vector was used as a control. siRNA against HNF1A and a scrambled negative control (si-NC) were obtained from Guangzhou IGE Biotechnology Ltd. According to the manufacturer's protocol, 2 μg plasmid/50 nM siRNA, 10 μl Lipofectamine 3000 (Invitrogen; Thermo Fisher Scientific, Inc.) and 500 μl Opti-MEM Medium (Gibco; Thermo Fisher Scientific, Inc.) were mixed gently and then incubated at room temperature for 15 min. The mixture was then slowly added to Panc-1 and MiaPaCa-2 cells. The cells transfected with plasmids/siRNA were incubated at 37˚C for 24 h, and then the culture medium was subsequently replaced with fresh DMEM supplemented with 10% FBS. Panc-1 and MiaPaCa-2 cells were harvested at 48 h after transfection. The siRNA sequences are listed in Table SII.

Western blotting. Panc-1 and MiaPaCa-2 cells were collected and lysed for 15 min on ice in RIPA buffer (Beyotime Institute of Biotechnology). Quantification of protein concentration was measured by bicinchoninic acid kit (Beyotime Institute of Biotechnology). A total of 30-50 μg protein was loaded per lane, separated by SDS-PAGE on 8-12% gels and transferred to 0.45-μm polyvinylidene difluoride (PVDF) membranes (Immobilon-P; MilliporeSigma). Subsequently, 5% skim milk (cat. no. 70166; Sigma-Aldrich; Merck KGaA) was used to block PVDF membranes for 1 h at room temperature. The membranes were incubated with primary antibodies overnight at 4˚C. Horseradish peroxidase-conjugated secondary antibodies were then used to incubate membranes at room temperature for 1 h. Protein expression was detected using an enhanced chemiluminescence detection system (Thermo Fisher Scientific, Inc.). The following primary antibodies were used: Rabbit anti-human HNF1A (1:1,000; cat. no. ab96777; Abcam), 53BP1 (1:1,000; cat. no. ab87097; Abcam), mouse anti-human GAPDH (1:2,000; cat. no. abs830030; Absin Bioscience, Inc.) The secondary antibodies were goat anti-rabbit IgG-HRP (1:10,000; abs20002) and goat anti-mouse IgG-HRP (1:10,000; cat. no. abs20001) (both from Absin Bioscience, Inc.).

Immunofluorescence staining. Panc-1 and MiaPaCa-2 cells were cultured in 6-well plates overnight. Cells were fixed in 4% paraformaldehyde for 10 min at room temperature and permeabilized with 0.1% Triton X-100 (Thermo Fisher Scientific, Inc.) for 15 min. After blocking with 5% bovine serum albumin (Beyotime Institute of Biotechnology) at room temperature for 60 min, cells were incubated with the following antibodies overnight at 4˚C: HNF1A (1:1,000; cat. no. ab96777; Abcam), γ-H2AX (1:1,000; cat. no. ab81299; Abcam). The cells were then incubated for 1 h in the dark at room temperature with the following secondary antibodies: Goat Anti-Rabbit IgG H&L (Alexa Fluor® 488) (1:2,000; cat. no. ab150077; Abcam) Subsequently, the cells were stained with DAPI (5 μg/ml; Beyotime Institute of Biotechnology) for 5 min at room temperature. The results were examined by laser scanning confocal microscopy (Leica Microsystems GmbH).

Cell proliferation assay. Panc-1 and MiaPaCa-2 were seeded in 96-well plates in duplicate at 3,000 cells/well. Oxaliplatin (5 μM)/cisplatin (5 μM; cat. no. S1166; Selleck Chemicals)/carboplatin (4 μM; cat. no. S1215; Selleck Chemicals) was added to the cells after 24 h and incubated for 4 days. According to the manufacturer's protocol, cell proliferation was determined daily using the Cell Counting Kit-8 (CCK-8) assay (cat. no. K1018; APExBIO Technology LLC) over 4 days. The absorbance was measured at 450 nm using a multiwell plate reader (Spark; Tecan Group, Ltd.).

Colony formation assay. Panc-1 and MiaPaCa-2 (2,000/well) were seeded in 6-well plates and treated with oxaliplatin (5 μM)/cisplatin (5 μM)/carboplatin (4 μM) at 37˚C for 48 h. The colonies were fixed for 15 min with 4% paraformaldehyde at room temperature and stained for 10 min with 0.25% crystal violet at room temperature after 2 weeks of incubation. The visible colonies (containing >50 cells) were counted and images were captured under an optical microscope.

Sphere formation assay. MiaPaCa-2 and Panc-1 cells (1,000 cells/well) were plated in 96-well extremely low attachment plates (Corning, Inc.) and treated with oxaliplatin (5 μM)/cisplatin (5 μM)/carboplatin (4 μM) at 37˚C for 48 h. Fibroblast growth factor (20 ng/ml), human recombinant epidermal growth factor (20 ng/ml) and serum substitute B27 (1X) were mixed into serum-free DMEM/F-12 and were added to each well (all from Invitrogen; Thermo Fisher Scientific, Inc.). The number of spheres >50 mm in diameter was counted under a light microscope after 2 weeks of incubation at 37˚C and 5% CO_2.

Annexin V/PI apoptosis assay. Panc-1 or MiaPaCa-2 cells were treated with 5 μM oxaliplatin for 48 h. The cells were stained with an Annexin V-PI staining kit (cat. no. BMS500FI;

eBioscience; Thermo Fisher Scientific, Inc.) to detect apoptosis. After being harvested, the cells were resuspended in FITC-conjugated Annexin V binding solution for 15 min at 37˚C and then stained with PI at room temperature for 5 min. Within 1 h, flow cytometry was performed using a FACSCanto II instrument (BD Biosciences) and FlowJo V10.0.7 software (FlowJo LLC).

Neutral comet assay. After treatment of MiaPaCa-2 and Panc-1 cells ($2x10^5$) with 5 μM oxaliplatin for 1 h at room temperature, time-lapse imaging was performed. A comet assay kit (cat. no. 4250-050-K; Trevigen, Inc.) was used in accordance with the manufacturer's instructions. SYBR gold stain kit (cat. no. S11494; Invitrogen; Thermo Fisher Scientific, Inc.) was used to stain the samples for 45 min at room temperature, which were observed under an Olympus FluoView 500 fluorescence microscope. The images were analyzed using CASP software (version no. 2013062811125300; Beijing Bio-launching Technologies Co., Ltd.).

pimEJ5-GFP reporter and pDR-GFP reporter assays. Transfection of MiaPaCa-2 and Panc-1 cells ($4x10^4$) with pimEJ5-GFP (ID 44026; Addgene, Inc.) or pDR-GFP (ID 26475; Addgene, Inc.) plasmids was performed using Lipofectamine 3000. According to the manufacturer's protocol, 1 μg plasmid, 10 μl Lipofectamine 3000 and 500 μl Opti-MEM were mixed gently and then incubated at room temperature for 15 min. The mixture was then slowly added to Panc-1 and MiaPaCa-2 cells. After incubating at 37˚C for 24 h, the culture medium was subsequently replaced with fresh DMEM supplemented with 10% FBS. Puromycin (2 μg/ml; MedChemExpress) was used to select stable clones of MiaPaCa-2 and Panc-1 cells that expressed pimEJ5-GFP or pDR-GFP. MiaPaCa-2 and Panc-1 cells that stably expressed pimEJ5-GFP or pDR-GFP were transfected with pCBASceI (I-SceI) plasmids (Addgene plasmid no. 26477; Addgene, Inc.) using Lipofectamine 3000 according to the aforementioned protocol. The GFP-positive cells were analyzed by FACSCanto II instrumentand FlowJo V10.0.7 software 48-72 h after transfection. A pair of plasmids carrying pimEJ5-GFPand pDR-GFPwere provided by Dr Jeremy Stark.

Chromatin immunoprecipitation (ChIP) assay. For 10 min at 37˚C, 1% formaldehyde was used to cross-link the proteins of Panc-1 cells. ChIP experiments were carried out using an anti-HNF1A antibody (5 μl/1 mg total protein; cat. no. ab96777; Abcam), with ChIP-grade rabbit IgG (1 μg/ml; cat. no. ab171870; Abcam) used as a negative control. ChIP assays were performed using an EZ-Magna ChIP Chromatin Immunoprecipitation kit (cat. no. 17-408. MilliporeSigma) according to the manufacturer's instructions. Immunoprecipitated DNA was analyzed by qPCR as aforementioned.

53BP1 promoter deletion constructs and luciferase reporter assay. The 53BP1 promotor deletion constructs were generated by Guangzhou IGE Biotechnology Ltd. Predictive binding site mutagenesis of the 53BP1 promotor was performed using a Quick Change Site-Directed Mutagenesis kit (Agilent Technologies, Inc.). Subsequently, the luciferase reporter plasmids [pGL3-53BP1, pGL3-53BP1-P (-5000-+200), pGL3-53BP1-P (-4000-+200), pGL3-53BP1-P (-3000-+200), pGL3-53BP1-P (-2000-+200), pGL3-53BP1-P (-1000-+200), pGL3-53BP1-P (+1-+200), pGL3-basic; Guangzhou IGE Biotechnology Ltd.] containing the 53BP1 promoter deletions were cotransfected with the HNF1A overexpression vector or empty vector into Panc-1 cells ($3x10^5$ cells) using 1 μl Lipofectamine 3000 at 37˚C for 24 h. A total of 24 h after transfection, the cells were collected, washed, and harvested for firefly and Renilla luciferase assays (cat. no. 16816; Thermo Fisher Scientific, Inc.).

Animal experiments. For orthotopic xenograft models, the BALB/c nude mice (female; age, 4-6 weeks; body weight, 18-20 g; Shulaibao Biotech) were housed at 5 per cage under specific pathogen-free conditions (temperature, 21±2˚C; humidity, 40-60%; 12-h light/dark cycle; free access to standard sterile food and water), and were randomly divided into the following three groups (n=5/group): i) luc-Panc-1 cells/empty vector, ii) luc-Panc-1 cells/HNF1A and iii) luc-Panc-1 cells/53BP1. Full-length HNF1A and 53BP1 were subcloned into pCDH-PGK-luciferase-EF1a-mcherry-T2a-puro vector (Guangzhou IGE Biotechnology Ltd.) and an empty vector was used as a control. The plasmids (2 μg) were transfected into Panc-1 cells using Lipofectamine 3000 according to the manufacturer's protocol. After 24 hours, the culture medium was replaced with fresh DMEM supplemented with 10% FBS. Puromycin (2 μg/ml; MedChemExpress) was used to select stable clones of Panc-1 cells that expressed HNF1A or 53BP1. A total of 48-72 h after transfection, the cells were harvested for mouse experiments. BALB/c nude mice were anesthetized with isoflurane inhalation (4-5% induction, 1-2% maintenance). A 1-cm left subcostal incision was made to expose the pancreas, which was injected with a 50-μl PBS suspension of luc-Panc-1 cells using a 30-G needle. Monofilament sutures were used to close the wound following orthotopic implantation. In a 15-day treatment period, oxaliplatin (5 mg/kg) was administered intraperitoneally once every 3 days, followed by IVIS imaging and tumor removal. D-Luciferin (150 mg/kg; cat. no. 161055-47-6; MilliporeSigma) and potassium salt (40902ES01; Shanghai Yeasen Biotechnology Co. Ltd.) were injected intravenously during the IVIS study, and orthotopic fluorescence images were recorded *in vivo* using an FXPRO system (Bruker Corporation). At each time point in the *in vivo* study, the mice were assessed by investigators who were blinded to the group allocation. All of the mice were sacrificed 30 days later.

A patient-derived xenograft (PDX) model was developed by propagating primary tumor specimens obtained from the aforementioned patients with oxaliplatin-resistant PDAC as subcutaneous tumors in 4-week-old NOD-SCID IL-2 receptor γ-null mice (F1, n=5/group; female; age, 4-6 weeks; body weight, 18-20 g; Shulaibao Biotech) were housed at 5 per cage under specific pathogen-free conditions (temperature, 21±2˚C; humidity, 40-60%; 12-h light/dark cycle; free access to standard sterile food and water). The NOD-SCID IL-2 receptor γ-null mice were anesthetized with 1% sodium pentobarbital (intraperitoneal injection, 30 mg/kg). The xenografts from F1 were implanted into other mice (F2) after separating them into small pieces. When the tumor volumes reached 1,500 mm^3,

they were excised, cut into small pieces again and transplanted into other mice (F3). A combination of AVV virus (Guangzhou IGE Biotechnology Ltd.) and oxaliplatin chemotherapy (intraperitoneal injection, 10 mg/kg) was administered when the xenograft volume reached ~200 mm^3. Throughout the treatment period, tumor volume was monitored every week. All of the mice were sacrificed 30 days later and IHC was performed on each tumor.

All mice were maintained in a specific pathogen-free environment. When reaching the following humane endpoints, the mice were euthanized: i) Tumor burden was >10% of body weight, and the diameter of tumor was >20 mm; ii) tumor ulceration, infection or necrosis was observed; iii) tumor interferes with eating or walking; iv) rapid weight loss (loss of 15-20% of original weight). Notably, none of these endpoints were reached during the experiments. Animal health and behavior were monitored twice a day (at the beginning and end of the day) by an experienced individual. The mice were euthanized by cervical dislocation under anesthesia (1% sodium pentobarbital intraperitoneal injection, 30 mg/kg). A comprehensive judgment on death was made by observing signs of respiration, heartbeat, and pupil and nerve reflexes. Animal experiments were conducted according to guidelines approved by the Animal Experimental Research Ethics Committee of South China University of Technology (Guangzhou, China; approval no. 2021042).

Database analysis. To predict the binding site of HNF1A at the 53BP1 promoter region, the JASPAR database (https://jaspar.genereg.net/) was used.

Statistical analysis. SPSS version 20.0 software (IBM Corp.) was used to conduct all statistical analyses. All experiments were repeated at least three times. For parametric data, one way ANOVA with a Tukey's post-hoc test or unpaired Student's t-test was used. Unless otherwise stated, all values are expressed as the mean ± standard deviation. Kaplan-Meier method was used to assess differences in patient survival and the log-rank test was applied to analyze the data. Spearman's correlation analysis was used for the correlation analysis. $P<0.05$ was used to indicate a statistically significant difference.

Results

HNF1A expression is associated with oxaliplatin resistance in PDAC tissues and cell lines. Given that HNF1A is a critical suppressor of chemotherapy resistance in pancreatic cancer (14), the mRNA expression levels of HNF1A were detected in 76 patients with PDAC who accepted platinum-based chemotherapy. The results demonstrated that the expression levels of HNF1A were reduced in oxaliplatin-resistant patients compared with those in oxaliplatin-sensitive patients which were described in the methods (Fig. 1A). In addition, significantly lower expression levels of HNF1A were detected in oxaliplatin-resistant patients compared with those in oxaliplatin-sensitive patients, as determined by western blotting and IHC (Fig. 1B and C). Those with low HNF1A expression levels, according to RT-qPCR (cut-off according to the median expression level, there were 38 patients in the low HNF1A expression group and 38 in the high HNF1A expression group), had poorer PFS than those with high HNF1A expression levels (Fig. 1D).

Panc-1-R and MiaPaCa-2-R cells were treated with escalating concentrations of oxaliplatin *in vitro*. Panc-1 and MiaPaCa-2 cells were repeatedly stimulated in this manner until proliferation was no longer inhibited. As shown by the elevated IC_{50} values, Panc-1-R and MiaPaCa-2-R cells responded poorly to oxaliplatin compared with the parental cells (Fig. 1E). To clarify the relationship between HNF1A expression and oxaliplatin chemotherapy resistance, the mRNA and protein expression levels of HNF1A were detected in oxaliplatin-resistant and oxaliplatin-sensitive cells. RT-qPCR, western blotting and immunofluorescence assays indicated that the expression levels of HNF1A were markedly lower in the Panc-1-R and MiaPaCa-2-R cell lines compared with those in the oxaliplatin-sensitive cell lines (Fig. 1F-I).

HNF1A mediates platinum-based drug resistance in PDAC cell lines in vitro. To explore the role of HNF1A in oxaliplatin, cisplatin and carboplatin resistance, HNF1A was overexpressed or depleted in Panc-1 and MiaPaCa-2 cells. (Fig. S1A-D). HNF1A overexpression decreased the proliferation rate of Panc-1 and MiaPaCa-2 PDAC cells, as confirmed by the CCK-8 cytotoxicity assay. Conversely, silencing HNF1A enhanced platinum-based drug resistance in PDAC cells (Figs. 2A and B, S2A and B, and S3A and B). After exposure to platinum-based drugs, PDAC cells overexpressing HNF1A had a lower survival rate than control cells, as shown by colony formation assays, whereas HNF1A knockdown enhanced their survival (Figs. 2C and D, S2C and D, and S3C and D). Cancer stem cells have a pivotal role in chemoresistance (18). Notably, HNF1A overexpression in PDAC cells significantly reduced the self-renewal ability of the cells, as demonstrated by a sphere formation assay. By contrast, HNF1A knockdown significantly attenuated this effect (Figs. 2E and F, S2E and F, and S3E and F). Additionally, overexpression of HNF1A in tumor cells promoted cell early and late apoptosis under oxaliplatin treatment conditions, as determined by flow cytometry (Figs. 2G and S4A). Conversely, knockdown of HNF1A in PDAC cells markedly reversed this effect (Figs. 2H and S4B).

HNF1A switches HR to NHEJ. To determine the mechanism by which HNF1A downregulation mediates oxaliplatin resistance in PDAC cells, the present study detected whether DSB repair was altered by HNF1A. A neutral comet assay was performed and the expression levels of γH2AX were detected to assess damage to the genetic material (DSBs). Longer comet tails were present in the HNF1A-overexpressing groups, whereas HNF1A knockdown shortened the lengths of the comet tails following treatment with oxaliplatin, as determined by the neutral comet assay (Fig. 3A and B). In addition, following oxaliplatin treatment, the HNF1A-overexpressing groups had higher levels of γH2AX than the control group, indicating a higher number of DSBs. However, the expression levels of γH2AX were lower in the HNF1A knockdown group compared with in the si-NC group (Fig. 3C and D).

NHEJ and HR are the main pathways for DSB repair (19). To explore the effect of HNF1A on NHEJ and HR, the pimEJ5-GFP and pDR-GFP reporters were stably transfected into PDAC cells. The percentage of GFP-positive PDAC

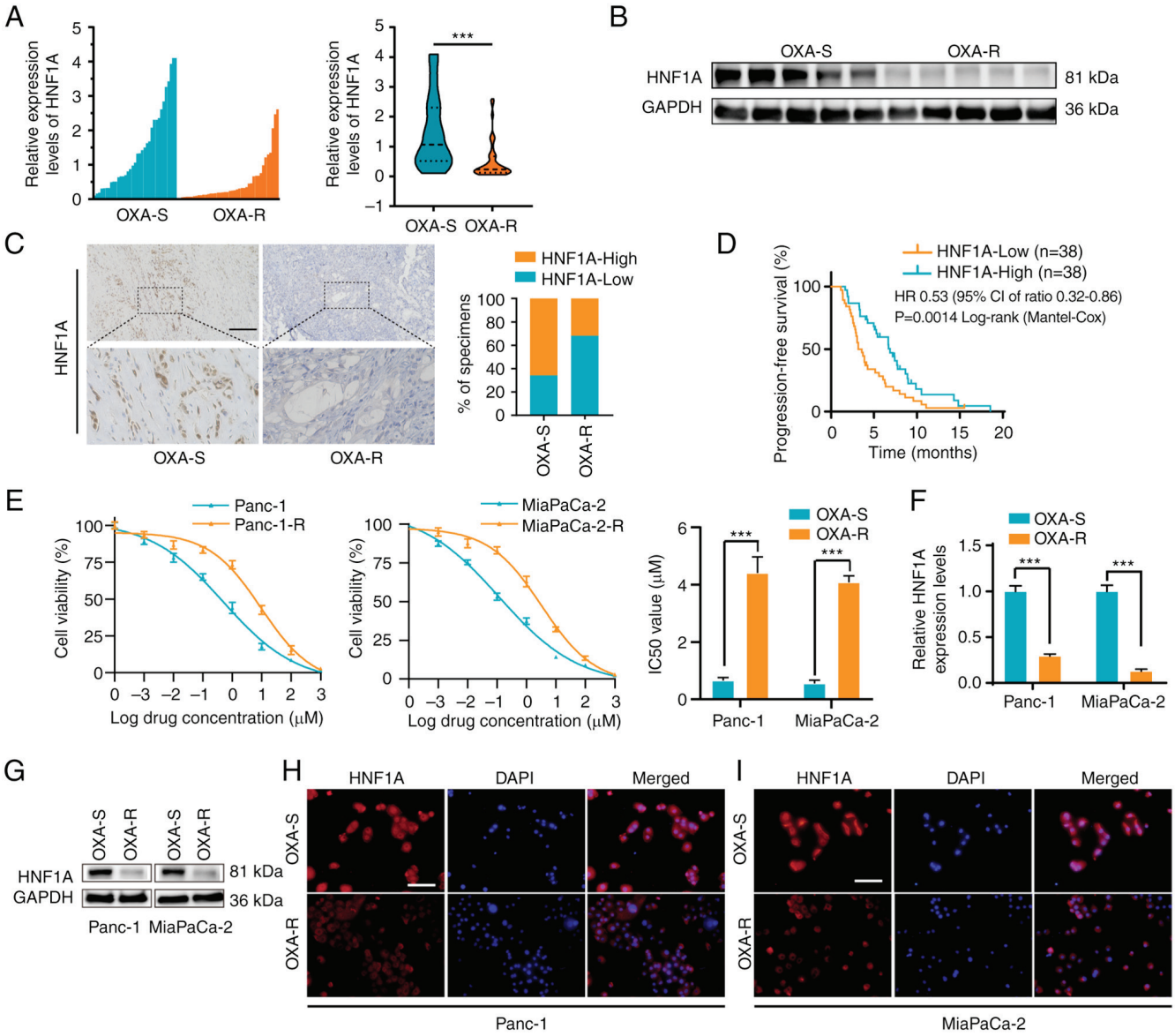

Figure 1. HNF1A expression is associated with OXA resistance in PDAC tissue and cell lines (A) Reverse transcription-quantitative PCR analysis of HNF1A expression in OXA-S (n=35) and OXA-R (n=41) PDAC tissues. (B) Western blot analysis of HNF1A in PDAC tissue from ox OXA-S and OXA-R patients. (C) Immunohistochemistry analysis of HNF1A in OXA-S and OXA-R PDAC tissues. Scale bars, 50 μm. (D) Survival of 76 patients with PDAC treated with platinum-based chemotherapy who had high or low HNF1A expression was analyzed based on Kaplan-Meier curves. (E) Dose-response curves were constructed for Panc-1 and MiaPaCa-2 cells to determine the IC_{50} of OXA. (F) HNF1A mRNA expression levels in OXA-S and OXA-R Panc-1 and MiaPaCa-2 cells. (G) Western blot analysis of HNF1A protein expression in each group. Representative immunofluorescence images of HNF1A in OXA-S and OXA-R (H) Panc-1 and (I) MiaPaCa-2 cells. Scale bars, 50 μm. The results are shown as the mean ± SD. ***P<0.001. HNF1A, hepatocyte nuclear factor 1 homeobox A; OXA, oxaliplatin; OXA-R, OXA-resistant; OXA-S, OXA-sensitive; PDAC, pancreatic ductal adenocarcinoma.

cells post-transfection with the pDR-GFP reporter or the pimEJ5-GFP reporter represented HR repair efficiency and NHEJ repair efficiency, respectively. HNF1A overexpression significantly suppressed HR-dependent DSB repair and promoted NHEJ-dependent DSB repair, whereas HNF1A knockdown had the opposite effect (Figs. 3E-H and S5A-D).

HNF1A regulates 53BP1 expression by binding to the 53BP1 promoter. To further reveal the downstream target of HNF1A in mediating HR/NHEJ, the mRNA expression levels of the key factors in HR and NHEJ were detected. Notably, only the mRNA expression levels of 53BP1 were significantly upregulated following overexpression of HNF1A in PDAC Panc-1 and MiaPaCa-2 cells (Fig. 4A and B). In addition, western blotting confirmed that HNF1A overexpression markedly increased the protein expression levels of 53BP1 (Fig. 4C). Given that HNF1A is known as a transcriptional activator, a ChIP assay was performed to determine whether HNF1A transcriptionally upregulated 53BP1. The results demonstrated that HNF1A interacted with the 5' regulatory region of 53BP1 at the -3 kb location (from the transport start site) instead of the 5' regulatory regions at the -2, -1, -4 and -5 kb locations (Fig. 4D). Furthermore, a series of 53BP1 promoter deletion reporter constructs were generated, and luciferase assays showed that the -3 to -5 kb region of the 53BP1 promoter led to a significant increase in transcriptional activity in HNF1A-overexpressing tumor cells (Fig. 4E). Using JASPAR, it was predicted that HNF1A may bind to the promoter region of 53BP1 from

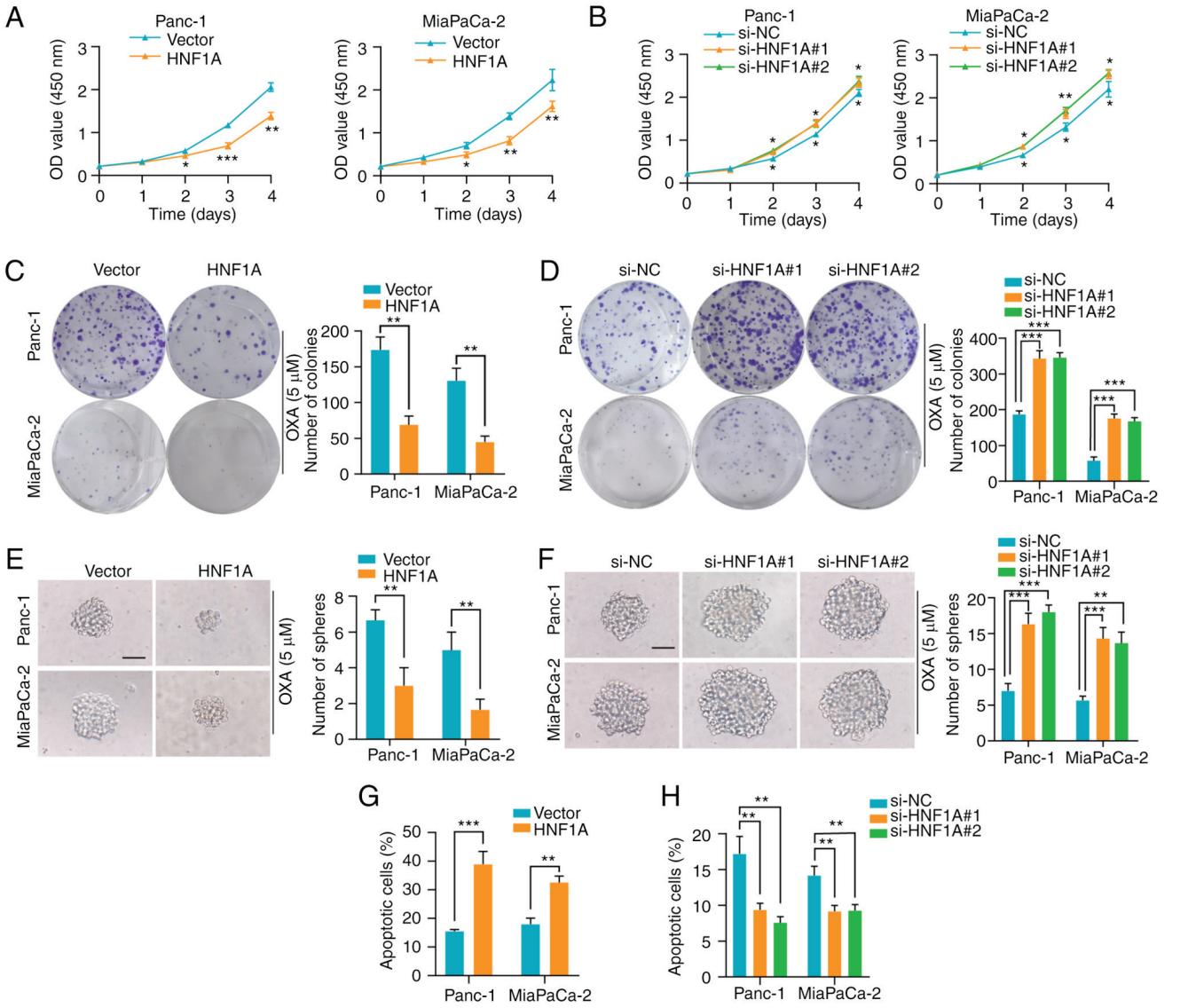

Figure 2. HNF1A mediates OXA resistance in pancreatic ductal adenocarcinoma cell lines *in vitro*. (A) Proliferation of Panc-1 and MiaPaCa-2 cells overexpressing HNF1A under OXA treatment (5 μM), as determined using the Cell Counting Kit-8 assay. *P<0.05, **P<0.01 and ***P<0.001 vs. Vector. (B) Proliferation of Panc-1 and MiaPaCa-2 cells following knockdown of HNF1A under OXA treatment (5 μM), as determined using the Cell Counting Kit-8 assay. *P<0.05 and **P<0.01 vs. si-NC. Representative images of the colony formation of Panc-1 and MiaPaCa-2 cells (C) post-HNF1A plasmid transfection or (D) post-si-HNF1A transfection and under OXA treatment (5 μM). Sphere formation assays showing Panc-1 and MiaPaCa-2 cell proliferation (E) post-HNF1A plasmid transfection or (F) post-si-HNF1A transfection and under OXA treatment (5 μM). Scale bars, 50 μm. OXA-induced (5 μM) apoptosis of Panc-1 and MiaPaCa-2 cells was examined through flow cytometry after (G) HNF1A plasmid or (H) si-HNF1A transfection. The results are shown as the mean ± SD. *P<0.05, **P<0.01 and ***P<0.001. HNF1A, hepatocyte nuclear factor 1 homeobox A; OXA, oxaliplatin; NC, negative control; si, small interfering.

-2,817 to -2,803 bp (5'-AATTAATCATTAAAT-3') (Fig. 4F). Luciferase assays showed that mutation of the predicted binding site in the 53BP1 promoter abrogated the increase in luciferase intensity induced by HNF1A overexpression (Fig. 4G). Collectively, these results indicated that HNF1A was bound to the specific promoter region (-2,817 to -2,803 bp) of 53BP1 and promoted 53BP1 expression to sensitize PDAC cells to chemotherapy.

53BP1 reverses the effects of HNF1A inhibition. The present study explored whether 53BP1 rescued the effect of HNF1A on oxaliplatin resistance. 53BP1was successfully overexpressed in Panc-1 and MiaPaCa-2 cells (Fig. S1E and F). The CCK-8 cytotoxicity and colony formation assays indicated that 53BP1 overexpression abrogated the promoting effect of HNF1A knockdown on tumor cells (Fig. 5A and B). In addition, the increase in tumor stemness induced by HNF1A knockdown was blocked by 53BP1 overexpression (Figs. 5C), and apoptosis resistance induced by HNF1A knockdown was also blocked by 53BP1 overexpression (Figs. 5D and S6). Consistently, neutral comet assays and γH2AX analysis revealed that 53BP1 overexpression weakened the enhancing effect of HNF1A knockdown on DNA repair efficiency (Fig. 5E and F). Furthermore, the pimEJ5-GFP reporter assay showed that the increase in the ratio of HR-dependent DSB repair caused by HNF1A knockdown was attenuated by 53BP1 overexpression (Figs. 5G and S7A). Similarly, the pDR-GFP reporter assay indicated that 53BP1 overexpression enhanced NHEJ-dependent DSB repair in HNF1A-depleted tumor cells (Figs. 5H and S7B).

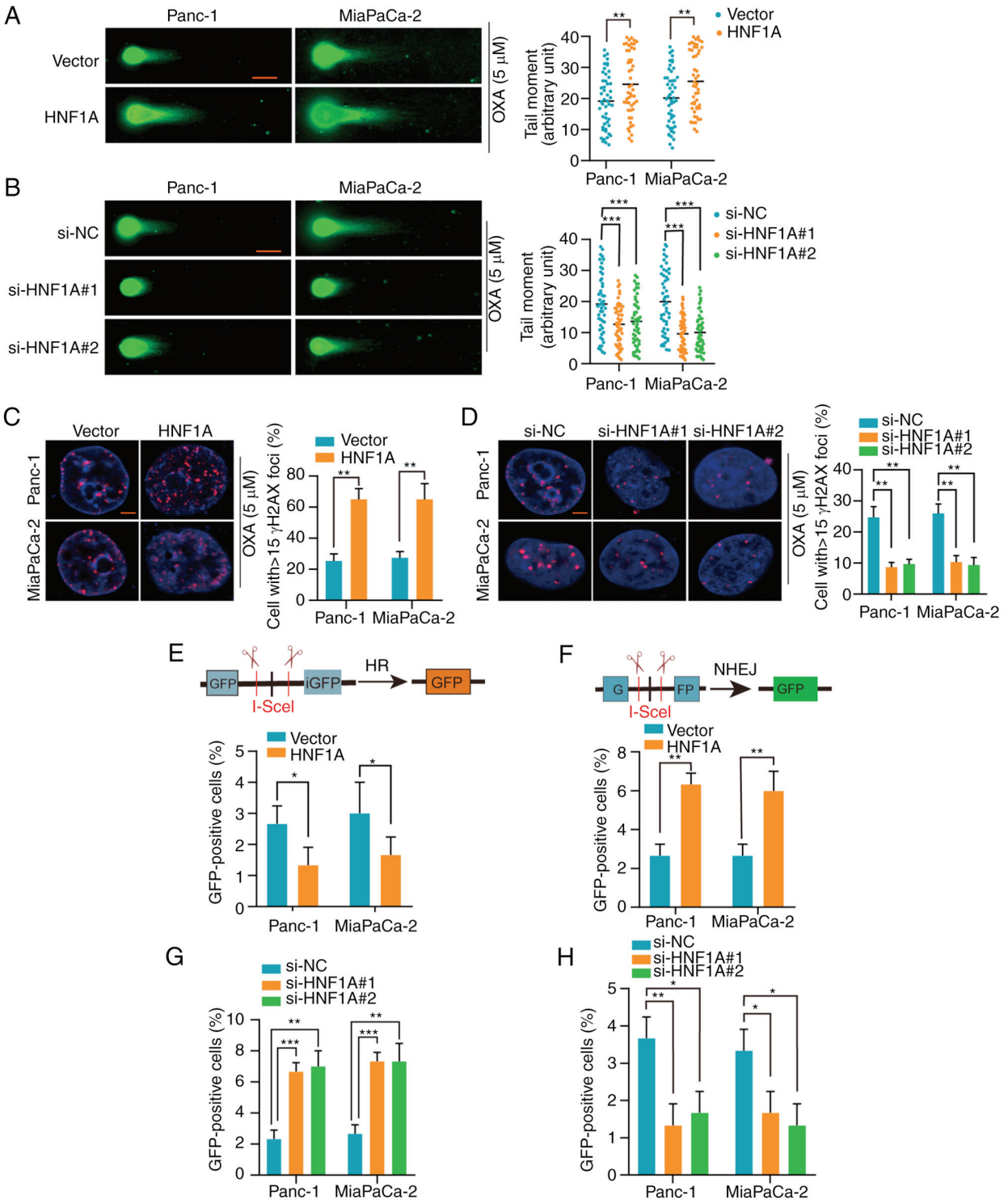

Figure 3. HNF1A switches HR to NHEJ. Neutral comet assay was used to measure the DNA damage caused by OXA (5 μM) in cells with (A) HNF1A overexpression or (B) HNF1A knockdown. Scale bar, 10 μm. Representative images of γH2AX-positive foci in Panc-1 and MiaPaCa-2 cells with (C) HNF1A overexpression or (D) HNF1A knockdown and treated with OXA (5 μM). Scale bar, 10 μm. Panc-1 and MiaPaCa-2 cells HR-mediated DNA repair efficiency was detected by the (E) pDR-GFP reporter assay and (F) pimEJ5-GFP reporter assay in vector and HNF1A-overexpressing groups. (G) Panc-1 and MiaPaCa-2 cells HR-mediated DNA repair efficiency was detected by the pDR-GFP reporter assay si-NC and si-HNF1A groups. (H) Panc-1 and MiaPaCa-2 cells NHEJ-mediated DNA repair efficiency was detected by the pimEJ5-GFP reporter assay in si-NC and si-HNF1A groups. The technical replicates were performed three times. The results are shown as the mean ± SD. *P<0.05, **P<0.01 and ***P<0.001. HNF1A, hepatocyte nuclear factor 1 homeobox A; HR, homologous recombination; NC, negative control; NHEJ, nonhomologous end joining; OXA, oxaliplatin; si, small interfering.

HNF1A loss promotes oxaliplatin resistance in vivo. For the *in vivo* experiments, the pancreases of nude mice were orthotopically implanted with the indicated luciferase-labeled Panc-1 cells, and oxaliplatin chemotherapy was administered 12 days after pancreatic implantation. The mice in the HNF1A-overexpression and 53BP1-overexpression groups exhibited lower fluorescence intensity in the pancreas and had smaller tumors than the control mice (Fig. 6A-C). IHC further

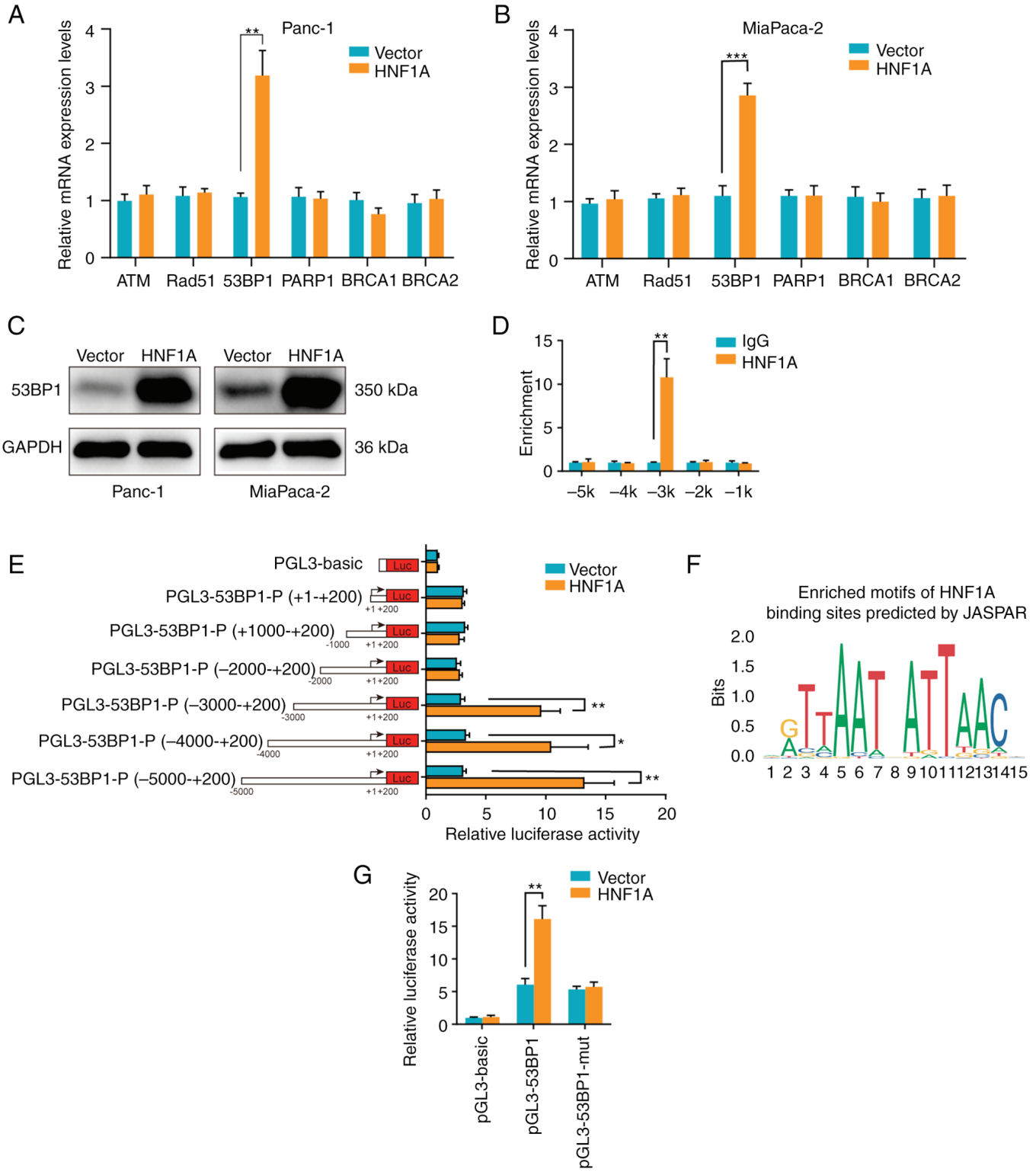

Figure 4. HNF1A regulates 53BP1 expression by binding to the 53BP1 promoter. Reverse transcription-quantitative PCR analysis of the key factors in HR or NHEJ (ATM, Rad51, 53BP1, PARP1, BRAC1 and BRAC2) in (A) Panc-1 and (B) MiaPaCa-2 cells. (C) Western blot analysis of the expression levels of 53BP1 in Panc-1 and MiaPaCa-2 cells. (D) Chromatin immunoprecipitation analysis of 53BP1 promoter occupancy by HNF1A in Panc-1 cells. (E) Luciferase reporter assays of Panc-1 cells overexpressing HNF1A transfected with reporter plasmids including sequential deletions in the 53BP1 promoter. (F) Schematic diagram of the potential HNF1A motif-binding locations in the promoter of 53BP1. (G) Luciferase reporter assays of wild-type or binding site-mutated HNF1A promoters in Panc-1 cells transfected with empty vector or HNF1A. The results are presented as the mean ± SD of three technical replicates. *P<0.05, **P<0.01 and ***P<0.001. 53BP1, p53-binding protein 1; HNF1A, hepatocyte nuclear factor 1 homeobox A.

confirmed that HNF1A/53BP1 markedly reduced γH2AX and Ki-67 expression (Fig. 6D).

To further simulate the situation in the human body, a PDX model was established. Animals were treated

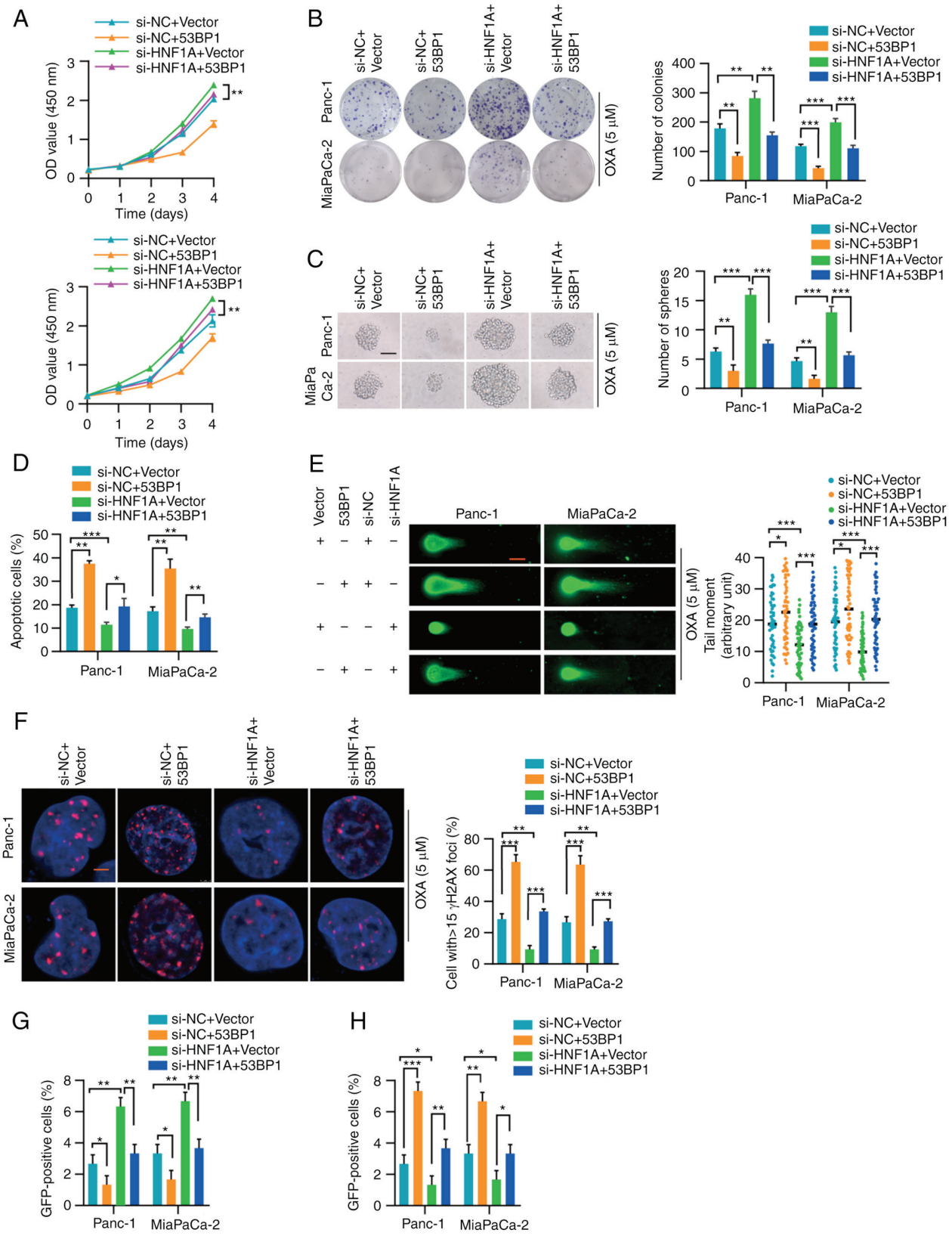

Figure 5. 53BP1 reverses the effect of HNF1A knockdown. (A) Proliferation of Panc-1 and MiaPaCa-2 cells with the indicated treatment was measured by Cell Counting Kit-8 assay. (B) Representative images and semi-quantification of colony formation in Panc-1 and MiaPaCa-2 cells treated with OXA (5 μM). (C) Representative images and semi-quantification of sphere formation in Panc-1 and MiaPaCa-2 cells with the indicated treatment under OXA incubation (5 μM). Scale bars, 50 μm. (D) Flow cytometry was performed to assess the apoptosis of Panc-1 and MiaPaCa-2 cells treated with OXA (5 μM). (E) Representative images and semi-quantification of the neutral comet assay in Panc-1 and MiaPaCa-2 cells. In total, 50 cells per group were counted. Scale bar, 10 μm. (F) Semi-quantification and representative images of γH2AX-positive foci in each group. More than 40 cells from each group were counted. (G and H) HR-mediated DNA repair efficiency was detected by the pimEJ5-GFP reporter assay, whereas NHEJ-mediated DNA repair efficiency was detected by the pDR-GFP reporter assay. Three independent replicates were performed. Data are expressed as the mean ± SD. *P<0.05, **P<0.01 and ***P<0.001. 53BP1, p53-binding protein 1; HNF1A, hepatocyte nuclear factor 1 homeobox A; HR, homologous recombination; NC, negative control; NHEJ, nonhomologous end joining; OXA, oxaliplatin; si, small interfering.

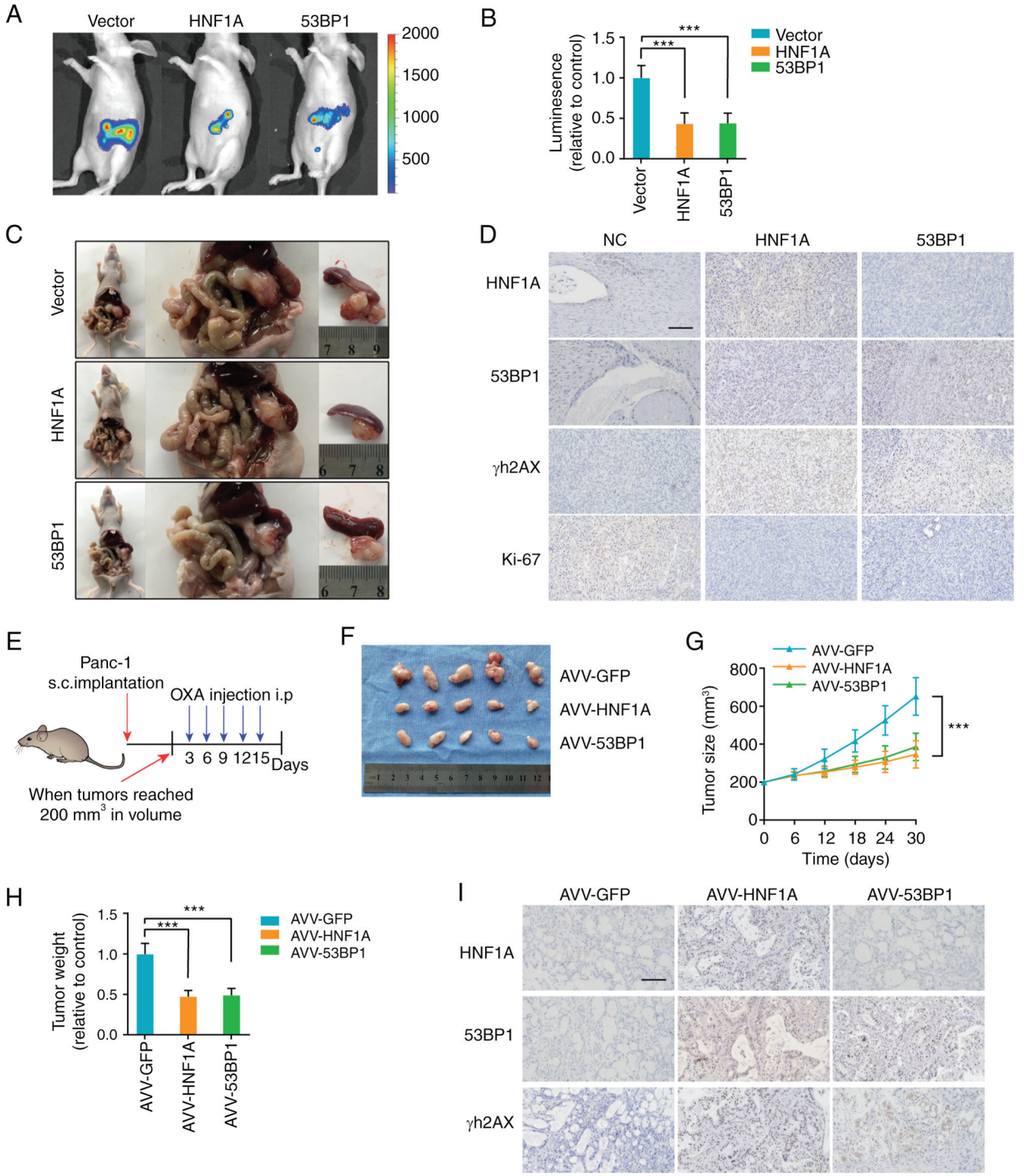

Figure 6. HNF1A knockdown promotes OXA resistance *in vivo*. (A) Representative IVIS images of an orthotopic xenograft model, n=5/group. (B) Calculation of the luminescence intensity of the orthotopic xenograft model. (C) Representative pancreatic tumor images of the orthotopic xenograft model. (D) Representative IHC images for HNF1A, 53BP1, γH2AX and Ki-67 in the orthotopic xenograft model. Scale bars, 50 μm. (E) Once the tumor volume reached 200 mm^3, the xenograft subcutaneous model received oxaliplatin (5 mg/kg) once every 3 days, n=5/group. Changes in (F and G) tumor volume and (H) weight were monitored. (I) Representative IHC images for HNF1A, 53BP1 and γH2AX in the patient-derived xenograft model. The results are presented as the mean ± SD. ***P<0.001, 53BP1, p53-binding protein 1; HNF1A, hepatocyte nuclear factor 1 homeobox A; IHC, immunohistochemistry; NC, negative control; OXA, oxaliplatin.

with oxaliplatin and AVVs (AVV-GFP, AVV-HNF1A, AVV-53BP1) when the tumor reached 200 mm^3 (Fig. 6E). The tumors of the AVV-HNF1A and AVV-53BP1 groups were substantially smaller and lighter than those in the AVV-GFP group (Fig. 6F-H). In addition, the data demonstrated that tumors from the AVV-HNF1A and AVV-53BP1 groups

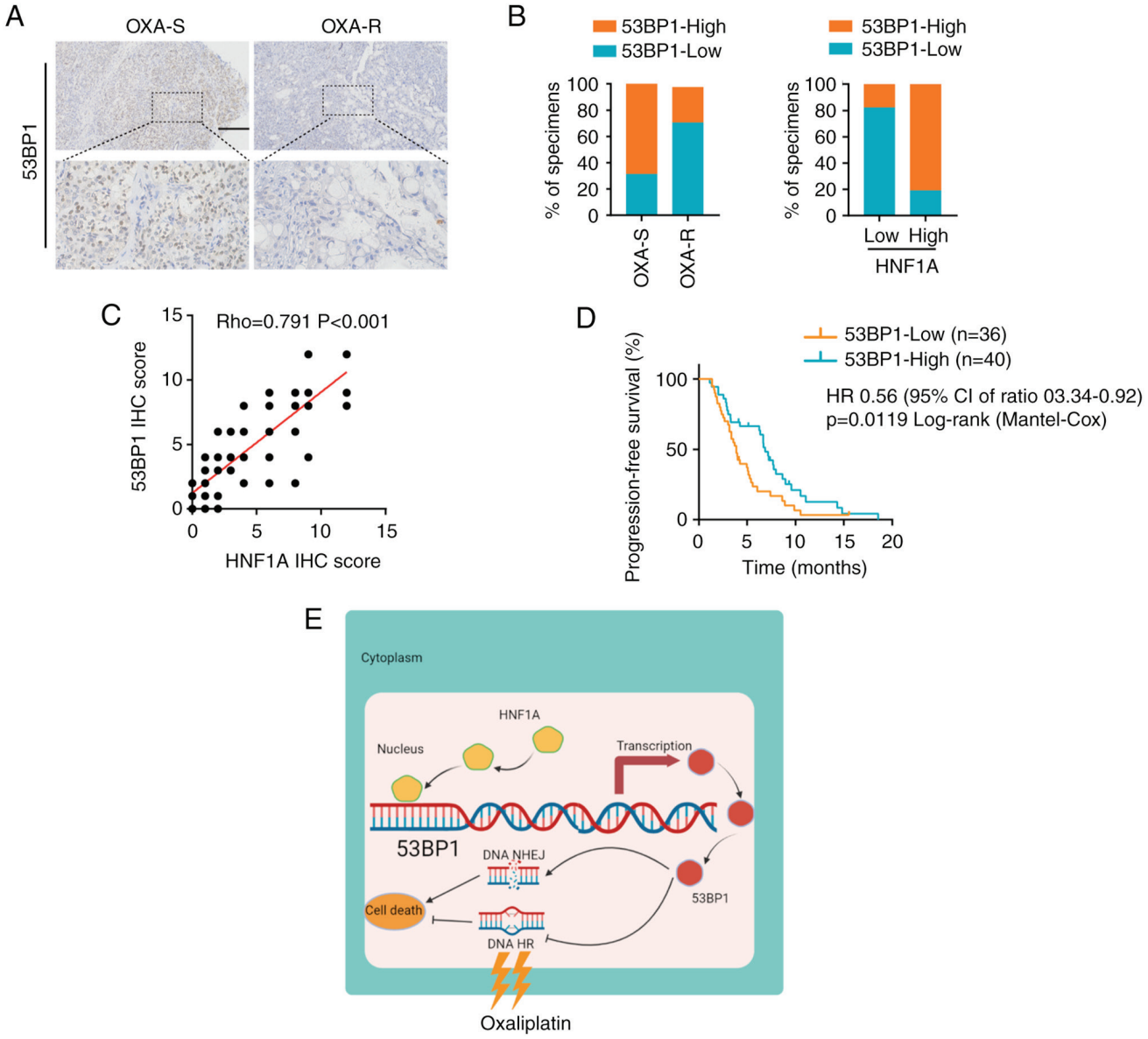

Figure 7. Clinical significance of the HNF1A/53BP1 axis in PDAC. (A) Immunohistochemistry analysis of 53BP1 in OXA-S and OXA-R PDAC tissues. Scale bars, 50 μm. (B) Semi-quantification of the percentage of OXA-S and OXA-R PDAC specimens with low or high 53BP1 expression. (C) Correlation between HNF1A expression and 53BP1 protein levels in PDAC tissues. (D) Kaplan-Meier curves of progression-free survival associated with 53BP1 expression evaluated by IHC in patients with PDAC who received platinum-based chemotherapy. (E) Graphical illustration of the mechanism by which HNF1A mediates 53BP1 activation in PDAC cells to reduce oxaliplatin resistance. 53BP1, p53-binding protein 1; HNF1A, hepatocyte nuclear factor 1 homeobox A; HR, homologous recombination; IHC, immunohistochemistry; NHEJ, nonhomologous end joining; OXA, oxaliplatin; OXA-R, OXA-resistant; OXA-S, OXA-sensitive; PDAC, pancreatic ductal adenocarcinoma.

exhibited a marked decrease in the positive rate of γH2AX staining (Fig. 6I). Collectively, these results support the idea that HNF1A transcriptionally activates 53BP1 expression and sensitizes tumors to oxaliplatin.

Clinical significance of the HNF1A/53BP1 axis in PDAC. To better understand the clinical significance of the HNF1A/53BP1 axis in oxaliplatin resistance, the expression levels of 53BP1 and HNF1A were examined in 76 patients with PDAC who received platinum-based chemotherapy. The findings revealed that the expression levels of 53BP1 were significantly lower in oxaliplatin-resistant patients compared with those in oxaliplatin-sensitive patients (Fig. 7A and B). Moreover, 53BP1 expression was positively correlated with HNF1A expression (Fig. 7C). Furthermore, patients with PDAC and low expression levels of 53BP1 had a significantly shorter PFS than those with high expression levels of 53BP1, as shown by Kaplan-Meier analysis (Fig. 7D). Overall, the present study indicated that HNF1A may have an important role in oxaliplatin resistance by regulating 53BP1 expression, and mediating HR and NHEJ imbalances in patients with PDAC (Fig. 7E).

Discussion

Pancreatic cancer is a lethal disease with a poor survival rate, due to a poor response to chemotherapy (20). Platinum-based chemotherapy is a first-line chemotherapy treatment for patients with advanced pancreatic cancer; however, the overall

response rate is only 30% worldwide (21). Our previous study reported that cancer-associated fibroblasts promote the acquired oxaliplatin resistance of pancreatic cancer cells via paracrine signaling (22). However, there are few studies on the inherent oxaliplatin resistance of pancreatic cancer tumor cells (23). The present study revealed that low HNF1A expression was associated with platinum-based chemotherapy resistance and a poor prognosis. Gain- and loss-of-function assays indicated that HNF1A serves an important role in oxaliplatin resistance by affecting DNA DSB repair. In addition, HNF1A was shown to mediate cisplatin and carboplatin resistance in PDAC cells, which expands the therapeutic value of HNF1A in platinum-based chemotherapy. Mechanistically, HNF1A directly binds to the 53BP1 promoter region and transcriptionally activates 53BP1 expression, which switches HR-dependent DNA repair to NHEJ-dependent DNA repair. Pancreatic cancer orthotopic and PDX models revealed the potential value of HNF1A as a therapeutic target for overcoming oxaliplatin resistance in pancreatic cancer.

Conflicting roles of HNF1A in anticancer drug resistance of different types of cancer have been reported. Fujino *et al (*16) and Wang *et al* (24) reported that HNF1A inhibition significantly reduced the proliferation and anticancer drug resistance of non-small cell lung cancer and colorectal cancer via glucose metabolism. Conversely, in another study, inhibition of HNF1A enhanced gemcitabine resistance by regulating multidrug resistance genes in pancreatic cancer (14). The present study revealed that HNF1A influenced the balance of HR and NHEJ to enhance the oxaliplatin sensitivity of PDAC *in vivo* and *in vitro*. It was hypothesized that the function of HNF1A may differ in different molecular subtypes of cancer (25). Germline HNF1A mutations have been linked to MODY3 through impaired insulin secretion and decreased β-cell mass (12,26). According to a genome-wide association study, genetic variants in the HNF1A locus predispose patients to PDAC (27). Kalisz *et al (*28) reported that KDM6A mutations led to HNF1A deficiency in non-classical PDAC (also defined as quasimesenchymal, basal and squamous-like PDAC). The present study revealed low expression of HNF1A in patients with oxaliplatin-resistant PDAC, which may be caused by HNF1A mutations. These observations and results indicated the value of HNF1A as a biomarker for guiding the use of platinum-based chemotherapy and even some targeted therapies.

Platinum-based chemotherapy resistance is an important obstacle in improving the prognosis of pancreatic cancer and is exemplified by a low objective response rate (29). Tumor cells repair double-strand breaks caused by platinum-based drugs via HR and NHEJ (30). Compared with NHEJ, HR-dependent DNA repair is more precise, and NHEJ-dependent DNA repair often causes genome instability and cell death (19,31). A recent clinical trial suggested that the combination of PARP inhibitors in patients with BRCA1/2 mutations greatly improved patient outcomes (32). A promising research direction involves the use of PARP inhibitors in tumor cells with HR deficiency. The combination of platinum-based therapy and PARP inhibitors may benefit patients with pancreatic cancer and high HNF1A expression, and requires further exploration.

The regulators 53BP1, ATM, Rad51, PARP1, BRCA1 and BRCA2 are important in DSB repair (29,33-35). The present study identified 53BP1 as the downstream target of HNF1A via RT-qPCR and western blotting. 53BP1 is a chromatin-binding protein, which regulates DSB repair by suppressing the nucleolytic resection of DNA termini (36). 53BP1 serves a crucial role in maintaining the balance of HR and NHEJ, which is important for genomic stability. The upstream regulatory mechanism of 53BP1 has attracted increasing attention. Parnandi *et al (*37) reported that Tudor-interacting repair regulator interacted with the 53BP1 Tudor domain and prevented its recruitment to DSBs (37). AMPK is directly associated with 53BP1 and phosphorylates it at Ser1317, promoting 53BP1 recruitment to DSBs (38). There is no evidence of 53BP1 transcriptional activation. Given that HNF1A is a known transcription factor, the present study demonstrated that HNF1A could directly enhance the transcription of 53BP1. ChIP and luciferase assays confirmed that HNF1A interacted with the 53BP1 promoter region. The present study provided a novel mechanism for regulating 53BP1, which may improve the understanding of DNA repair and oxaliplatin resistance. There are some limitations to the present study that could be addressed in future research. First, the clinical sample size was small, which limits the application of 53BP1 and HNF1A in clinical practice. The clinical value of HNF1A and 53BP1 should be further confirmed in a larger cohort in future studies. Second, further research is required before this may be of use clinically. Finally, the mechanism of HNF1A in mediating oxaliplatin was not fully clarified. Other regulatory mechanisms may exist, which require further study.

In conclusion, the present study suggested that the HNF1A/53BP1 axis is critical for oxaliplatin resistance in PDAC. Therefore, HNF1A may be a potential therapeutic target in patients with PDAC.

Acknowledgments

Not applicable.

Funding

This study was supported by grants from the National Natural Science Foundation of China (grant nos. 82203691 and 82072639), the Guangdong Science and Technology Department (grant no. 2021A1515011089), the Special Fund of 'Dengfeng Plan' of Guangdong Provincial People's Hospital, China (grant nos. KJ012019509 and DFJH2020027) and the National Key Clinical Specialty Construction Project (2021-2024, grant no. 2022YW030009).

Availability of data and materials

The datasets used and/or analyzed during the current study are available from the corresponding author on reasonable request.

Authors' contributions

RC, XW and SZ conceived the idea for the project, coordinated the research and modified the manuscript. RX, CH and YY conducted most of the experiments. RC and XW confirmed the authenticity of all the raw data. XZ, TLi and RH collected the clinical samples and information, and also performed some experiments. All authors have read and approved the final manuscript.

Ethics approval and consent to participate

This research was approved by the Ethical Committee of Guangdong Provincial People's Hospital (approval no. KY-H-2022-011-01). All of the patients provided written informed consent before the biopsy sample collection. Animal experiments were carried out according to guidelines approved by the Animal Experimental Research Ethics Committee of South China University of Technology (approval no. 2021042).

Patient consent for publication

Not applicable.

Competing interests

The authors declare that they have no competing interests.

References

1. Siegel RL, Miller KD and Jemal A: Cancer statistics, 2018. CA Cancer J Clin 68: 7-30, 2018.
2. Li D, Xie K, Wolff R and Abbruzzese JL: Pancreatic cancer. Lancet 363: 1049-1057, 2004.
3. Neoptolemos JP, Kleeff J, Michl P, Costello E, Greenhalf W and Palmer DH: Therapeutic developments in pancreatic cancer: Current and future perspectives. Nat Rev Gastroenterol Hepatol 15: 333-348, 2018.
4. Conroy T, Desseigne F, Ychou M, Bouché O, Guimbaud R, Bécouarn Y, Adenis A, Raoul JL, Gourgou-Bourgade S, de la Fouchardière C, *et al*: FOLFIRINOX versus gemcitabine for metastatic pancreatic cancer. N Engl J Med 364: 1817-1825, 2011.
5. Sohal DPS, Kennedy EB, Khorana A, Copur MS, Crane CH, Garrido-Laguna I, Krishnamurthi S, Moravek C, O'Reilly EM, Philip PA, *et al*: Metastatic pancreatic cancer: ASCO clinical practice guideline update. J Clin Oncol 36: 2545-2556, 2018.
6. Wattenberg MM, Asch D, Yu S, O'Dwyer PJ, Domchek SM, Nathanson KL, Rosen MA, Beatty GL, Siegelman ES and Reiss KA: Platinum response characteristics of patients with pancreatic ductal adenocarcinoma and a germline BRCA1, BRCA2 or PALB2 mutation. Br J Cancer 122: 333-339, 2020.
7. Iwabuchi K, Bartel PL, Li B, Marraccino R and Fields S: Two cellular proteins that bind to wild-type but not mutant p53. Proc Natl Acad Sci USA 91: 6098-6102, 1994.
8. Pontoglio M: Hepatocyte nuclear factor 1, a transcription factor at the crossroads of glucose homeostasis. J Am Soc Nephrol 11 (Suppl 16): S140-S143, 2000.
9. Odom DT, Zizlsperger N, Gordon DB, Bell GW, Rinaldi NJ, Murray HL, Volkert TL, Schreiber J, Rolfe PA, Gifford DK, *et al*: Control of pancreas and liver gene expression by HNF transcription factors. Science 303: 1378-1381, 2004.
10. Servitja JM, Pignatelli M, Maestro MA, Cardalda C, Boj SF, Lozano J, Blanco E, Lafuente A, McCarthy MI, Sumoy L, *et al*: Hnf1alpha (MODY3) controls tissue-specific transcriptional programs and exerts opposed effects on cell growth in pancreatic islets and liver. Mol Cell Biol 29: 2945-2959, 2009.
11. Li D, Duell EJ, Yu K, Risch HA, Olson SH, Kooperberg C, Wolpin BM, Jiao L, Dong X, Wheeler B, *et al*: Pathway analysis of genome-wide association study data highlights pancreatic development genes as susceptibility factors for pancreatic cancer. Carcinogenesis 33: 1384-1390, 2012.
12. Firdous P, Nissar K, Ali S, Ganai BA, Shabir U, Hassan T and Masoodi SR: Genetic testing of maturity-onset diabetes of the young current status and future perspectives. Front Endocrinol (Lausanne) 9: 253, 2018.
13. Luo Z, Li Y, Wang H, Fleming J, Li M, Kang Y, Zhang R and Li D: Hepatocyte nuclear factor 1A (HNF1A) as a possible tumor suppressor in pancreatic cancer. PloS One 10: e0121082, 2015.
14. Lu Y, Xu D, Peng J, Luo Z, Chen C, Chen Y, Chen H, Zheng M, Yin P and Wang Z: HNF1A inhibition induces the resistance of pancreatic cancer cells to gemcitabine by targeting ABCB1. EBioMedicine 44: 403-418, 2019.
15. Hoskins JW, Jia J, Flandez M, Parikh H, Xiao W, Collins I, Emmanuel MA, Ibrahim A, Powell J, Zhang L, *et al*: Transcriptome analysis of pancreatic cancer reveals a tumor suppressor function for HNF1A. Carcinogenesis 35: 2670-2678, 2014.
16. Fujino S, Miyoshi N, Ito A, Yasui M, Matsuda C, Ohue M, Uemura M, Mizushima T, Doki Y and Eguchi H: HNF1A regulates colorectal cancer progression and drug resistance as a downstream of POU5F1. Sci Rep 11: 10363, 2021.
17. Livak KJ and Schmittgen TD: Analysis of relative gene expression data using real-time quantitative PCR and the 2(-Delta Delta C(T)) method. Methods 25: 402-408, 2001.
18. Clarke MF, Dick JE, Dirks PB, Eaves CJ, Jamieson CH, Jones DL, Visvader J, Weissman IL and Wahl GM: Cancer stem cells-perspectives on current status and future directions: AACR Workshop on cancer stem cells. Cancer Res 66: 9339-9344, 2006.
19. Ceccaldi R, Rondinelli B and D'Andrea AD: Repair pathway choices and consequences at the double-strand break. Trends Cell Biol 26: 52-64, 2016.
20. Rahib L, Smith BD, Aizenberg R, Rosenzweig AB, Fleshman JM and Matrisian LM: Projecting cancer incidence and deaths to 2030: The unexpected burden of thyroid, liver, and pancreas cancers in the United States. Cancer Res 74: 2913-2921, 2014.
21. Meneses-Medina MI, Gervaso L, Cella CA, Pellicori S, Gandini S, Sousa MJ and Fazio N: Chemotherapy in pancreatic ductal adenocarcinoma: When cytoreduction is the aim. A systematic review and meta-analysis. Cancer Treat Rev 104: 102338, 2022.
22. Zhang X, Zheng S, Hu C, Li G, Lin H, Xia R, Ye Y, He R, Li Z, Lin Q, *et al*: Cancer-associated fibroblast-induced lncRNA UPK1A-AS1 confers platinum resistance in pancreatic cancer via efficient double-strand break repair. Oncogene 41: 2372-2389, 2022.
23. Chiu CF, Park JM, Chen HH, Mau CZ, Chen PS, Su YH, Chen HA, Liu YR, Hsieh TH, Chiu CC, *et al*: Organic cation transporter 2 activation enhances sensitivity to oxaliplatin in human pancreatic ductal adenocarcinoma. Biomed Pharmacother 153: 113520, 2022.
24. Wang J, Huang H and Liu F: DNAJC12 activated by HNF1A enhances aerobic glycolysis and drug resistance in non-small cell lung cancer. Ann Transl Med 10: 492, 2022.
25. Collisson EA, Bailey P, Chang DK and Biankin AV: Molecular subtypes of pancreatic cancer. Nat Rev Gastroenterol Hepatol 16: 207-220, 2019.
26. Farrelly AM, Wobser H, Bonner C, Anguissola S, Rehm M, Concannon CG, Prehn JH and Byrne MM: Early loss of mammalian target of rapamycin complex 1 (mTORC1) signalling and reduction in cell size during dominant-negative suppression of hepatic nuclear factor 1-alpha (HNF1A) function in INS-1 insulinoma cells. Diabetologia 52: 136-144, 2009.
27. Klein AP, Wolpin BM, Risch HA, Stolzenberg-Solomon RZ, Mocci E, Zhang M, Canzian F, Childs EJ, Hoskins JW, Jermusyk A, *et al*: Genome-wide meta-analysis identifies five new susceptibility loci for pancreatic cancer. Nat Commun 9: 556, 2018.
28. Kalisz M, Bernardo E, Beucher A, Maestro MA, Del Pozo N, Millán I, Haeberle L, Schlensog M, Safi SA, Knoefel WT, *et al*: HNF1A recruits KDM6A to activate differentiated acinar cell programs that suppress pancreatic cancer. EMBO J 39: e102808, 2020.
29. Laurini E, Marson D, Fermeglia A, Aulic S, Fermeglia M and Pricl S: Role of Rad51 and DNA repair in cancer: A molecular perspective. Pharmacol Ther 208: 107492, 2020.
30. Zhou J, Kang Y, Chen L, Wang H, Liu J, Zeng S and Yu L: The drug-resistance mechanisms of five platinum-based antitumor agents. Front Pharmacol 11: 343, 2020.
31. Brandsma I and Gent DC: Pathway choice in DNA double strand break repair: Observations of a balancing act. Genome Integr 3: 9, 2012.
32. Reiss KA, Mick R, O'Hara MH, Teitelbaum U, Karasic TB, Schneider C, Cowden S, Southwell T, Romeo J, Izgur N, *et al*: Phase II study of maintenance rucaparib in patients with platinum-sensitive advanced pancreatic cancer and a pathogenic germline or somatic variant in BRCA1, BRCA2, or PALB2. J Clin Oncol 39: 2497-2505, 2021.
33. Zhao Y, Simon M, Seluanov A and Gorbunova V: DNA damage and repair in age-related inflammation. Nat Rev Immunol 23: 75-89, 2022.

34. Ray Chaudhuri A and Nussenzweig A: The multifaceted roles of PARP1 in DNA repair and chromatin remodelling. Nat Rev Mol Cell Biol 18: 610-621, 2017.
35. Cleary JM, Aguirre AJ, Shapiro GI and D'Andrea AD: Biomarker-guided development of DNA repair inhibitors. Mol Cell 78: 1070-1085, 2020.
36. Noordermeer SM, Adam S, Setiaputra D, Barazas M, Pettitt SJ, Ling AK, Olivieri M, Álvarez-Quilón A, Moatti N, Zimmermann M, *et al*: The shieldin complex mediates 53BP1-dependent DNA repair. Nature 560: 117-121, 2018.
37. Parnandi N, Rendo V, Cui G, Botuyan MV, Remisova M, Nguyen H, Drané P, Beroukhim R, Altmeyer M, Mer G and Chowdhury D: TIRR inhibits the 53BP1-p53 complex to alter cell-fate programs. Mol Cell 81: 2583-2595.e2586, 2021.
38. Jiang Y, Dong Y, Luo Y, Jiang S, Meng FL, Tan M, Li J and Zang Y: AMPK-mediated phosphorylation on 53BP1 promotes c-NHEJ. Cell Rep 34: 108713, 2021.